compounds as well as in some doped semiconductor ferromagnets (as predicted in ref 31). The rise in these cases is due to the fact that magnetic fluctuations above the ordering temperature have a length scale on the order of the length scale of the conduction electrons (inverse of the Fermi wavevector, k_F), and this matching of length scales makes for more efficient scattering by the fluctuating magnetic ions. The change from ferromagnetism in $Ca_{14}MnBi_{11}$ and $Sr_{14}MnBi_{11}$ to antiferromagnetism in $Ba_{14}MnBi_{11}$ may be attributed to a decrease in k_F. The RKKY interaction oscillates in sign as k_FR is changed (where R is the distance between magnetic ions), so a decrease in k_F can cause a change in sign resulting in an antiferromagnetic ground state. The near-neighbor interaction may become small and antiferromagnetic, while the next-near-neighbor magnetic interaction at larger k_FR stays ferromagnetic and large. This is consistent with antiferromagnetic order appearing in a compound which has a positive θ.

The rise in resistivity as the temperature is lowered in $Ba_{14}MnBi_{11}$ is also reminiscent of heavy Fermion compounds where the excess scattering is due to the formation of a Kondo-like Fermi liquid state as the temperature is decreased. In this compound we have an ordered magnetic state at low T which is quite unlike the heavy Fermion compounds, but at the present time, we cannot rule out the influence of this type of conduction electron local moment interaction. Specific heat measurements on these compounds are currently underway to confirm our interpretation of the magnetic and transport properties.

Acknowledgment. We thank M. M. Olmstead for assistance with the structure determinations. The diffraction and computing equipment used in the structure determinations was purchased under National Science Foundation Grant CHE-8802721. We thank R. N. Shelton for use of the magnetometer and P. Klavins for assistance in resistivity measurements. Financial support from the University of California, Davis and the National Science Foundation, Division of Materials Research (DMR-8913831 and DMR-8913855) is gratefully acknowledged.

Registry No. $Ca_{14}Bi_{11}Mn$, 122744-53-0; $Bi_{11}MnSr_{14}$, 136939-46-3.

Supplementary Material Available: Additional diffraction and refinement data and anisotropic displacement parameters for $A_{14}MnBi_{11}$ (3 pages); tables of observed and calculated structure factors (16 pages). Ordering information is given on any current masthead page.

Binary Thin Films from Molecular Precursors. Role of Precursor Structure in the Formation of Amorphous and Crystalline FeB

Chang-Soo Jun and Thomas P. Fehlner*

Department of Chemistry and Biochemistry, University of Notre Dame, Notre Dame, Indiana 46556

Gary J. Long*

Department of Chemistry, University of Missouri—Rolla, Rolla, Missouri 65401

Received October 17, 1991. Revised Manuscript Received December 18, 1991

The ferraboranes $B_2H_6Fe_2(CO)_6$ and $[B_2H_4Fe_2(CO)_6]_2$ have been investigated as volatile precursors for the deposition of thin iron boride films with composition FeB. The thermal decomposition of $B_2H_6Fe_2(CO)_6$ on glass or aluminum substrates at 175–250 °C at pressures between 10^{-5} and 10^{-4} Torr results in the deposition of uniform, amorphous alloy films of average composition $Fe_{56}B_{44}$ contaminated with 2–4% carbon and oxygen impurities. Individual film thicknesses ranged from 1000 to 6000 Å. Mössbauer effect spectra of these films, when compared with those from films prepared from $HFe_3(CO)_9BH_4$, show that a random packing model does not apply and that local structure exists in these films. Crystallization of these films at 600 °C followed by X-ray diffraction and Mössbauer spectroscopic examination reveals the formation of two phases, namely, Fe_2B and FeB. Although the structures of these two phases are the same as those produced by conventional high-temperature routes, the latter phase exhibits significantly different Mössbauer behavior. Utilization of $[B_2H_4Fe_2(CO)_6]_2$ as a precursor yields films of similar composition. Crystallization leads again to Fe_2B and FeB and no significant differences in the films formed from the two different precursors were observed.

Introduction

In previous studies[1-3] we have demonstrated that $HFe_4(CO)_{12}BH_2$ and $HFe_3(CO)_9BH_4$ can serve as precursors for thin alloy films with Fe/B ratios tracking those in the molecular precursor clusters even if the actual Fe/B ratios are not precisely those of the precursor cores. In spite of complications caused by carbon and oxygen impurities derived in part from the cleavage of CO, many of the properties of these well-formed films, e.g., magnetic properties, approach those of $Fe_{80-x}B_{20+x}$ ribbons formed via rapid quenching techniques.[4] Rapid quenching techniques are restricted to materials with compositions near the eutectic composition, whereas the vapor deposition of main-group transition-element clusters has, in

(1) Fehlner, T. P.; Amini, M. M.; Zeller, M. V.; Stickle, W. F.; Pringle, O. A.; Long, G. J.; Fehlner, F. P. *Mater. Res. Soc. Symp. Proc.* **1989**, *131*, 413.

(2) Amini, M. M.; Fehlner, T. P.; Long, G. J.; Politowski, M. *Chem. Mater.* **1990**, *2*, 432.

(3) Thimmappa, B. H. S.; Fehlner, T. P.; Long, G. J.; Pringle, O. A. *Chem. Mater.* **1991**, *3*, 1148.

(4) Hasegawa, R. *Glassy Metals: Magnetic, Chemical, and Structural Properties*; CRC Press: Boca Raton, FL, 1983.

0897-4756/92/2804-0440$03.00/0

principle, no such limitation. Of course, there are other methods, such as sputtering, which also do not have this limitation.[5] However, the preferred direction of magnetization in the films or ribbons formed by the three different methods varies significantly.[2] Hence we have extended our earlier studies to the volatile $B_2H_6Fe_2(CO)_6$ (I)[6] and $[B_2H_4Fe_2(CO)_6]_2$ molecules (II),[7] both of which are

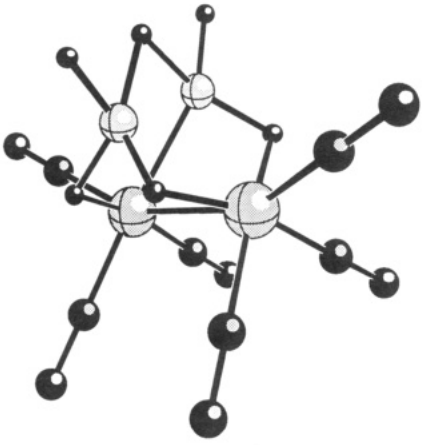

I

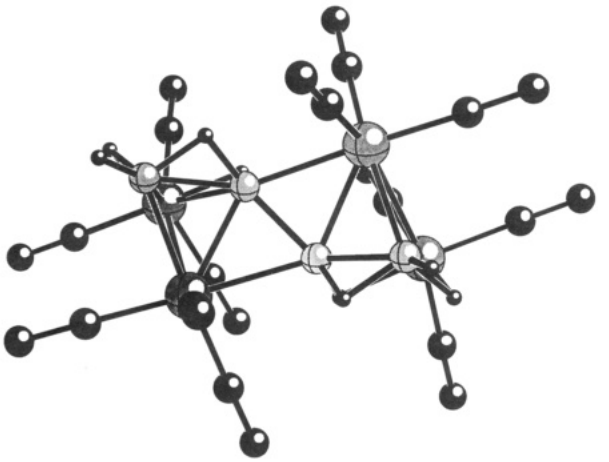

II

precursors for films with an ideal Fe/B ratio of 1. In both schemes the large and small, light balls represent Fe and B, respectively, the medium and small black balls represent C and H, respectively, and the remaining medium balls represent O. The significant structural differences between the two compounds allows one to address the question of whether the precursor cluster retains its integrity during the deposition process.

Metallaboranes may be viewed as potential sources of new metal borides.[8,9] An important aspect of these potential sources resides in the fact that metallaborane clusters yield amorphous borides at temperatures far lower than those required for the production of these refractory materials in crystalline form. Hence, the controlled crystallization of the amorphous materials constitutes a possible method for the isolation of new metastable crystalline forms of materials of previously known and unknown stoichiometry. This observation is particularly

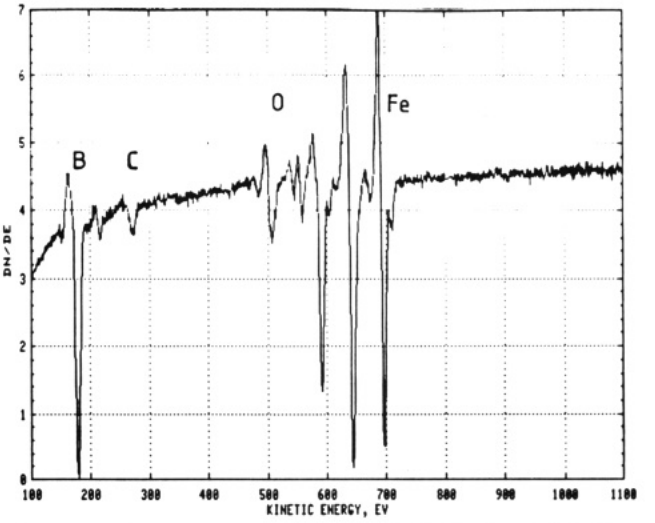

Figure 1. Auger spectrum ($dN(E)/E$) obtained at 3 kV of an amorphous film produced from the deposition of $B_2H_6Fe_2(CO)_6$ at 170 °C after sputtering ≈150 Å of the top surface of a 3000-Å-thick film on a glass substrate.

interesting in the context of FeB. Compounds with the stiochiometry MB are known to exhibit three principal structures, known as the "FeB", "CrB", and "MoB" type structures by virtue of the composition of the first characterized structure.[10] These structure types differ in a subtle manner in the way in which the common structural units are stacked. Indeed, there are both a high-temperature modification of HoSi with the "FeB" structure and a low-temperature modification with the "CrB" structure known.[11] Thus, it seemed possible that the crystallization of an amorphous FeB phase formed at low temperature might lead to more than one crystalline form; a form which may differ for the two different precursors.

Results

Composition. A typical Auger spectrum of a film formed from $B_2H_6Fe_2(CO)_6$ is shown in Figure 1. Both carbon and oxygen impurity levels are considerably below those found for $HFe_3(CO)_9BH_4$ and $HFe_4(CO)_{12}BH_2$ (5–10 and 10–15%, respectively).[12] Spectra were acquired under identical conditions from both the film and a standard of known composition which was mounted adjacent to the film. The standard was used to provide sensitivities for Fe, B, and C; however, both low-beam currents and slow sputtering rates were used to avoid boron loss during the Auger analysis.[12] After sputtering away between 50 and 100 Å of the contaminated surface layers, an average Fe/B ratio of 1.3 ± 0.1 was obtained at the lowest deposition temperature of 170 °C. This ratio increased with increasing temperature to a value of 1.7 at 250 °C. As observed in our previous work, a ratio above 1 implies the loss of some boron at the lowest temperature; a loss which increases with increasing temperature. The carbon and oxygen impurities ranged from 2 to 4% each.

Our previous work[3] on $HFe_3(CO)_9BH_4$-derived films suggested that a significant fraction of the film's carbon and oxygen impurities arose from an average of ≤0.5 trapped CO molecules per molecule of precursor. To promote decomposition just above the actual deposition surface and thereby increase the rate of CO escape, one

(5) Chien, C. L.; Musser, D.; Gyorgy, E. M.; Sherwood, R. C.; Chen, H. S.; Luborsky, F. E.; Walter, J. L. *Phys. Rev. B* **1979**, *20*, 283.
(6) Jacobsen, G. B.; Andersen, E. L.; Housecroft, C. E.; Hong, F.-E.; Buhl, M. L.; Long, G. J.; Fehlner, T. P. *Inorg. Chem.* **1987**, *26*, 4040.
(7) Jun, C.-S.; Meng, X.; Haller, K. J.; Fehlner, T. P. *J. Am. Chem. Soc.* **1991**, *113*, 3603.
(8) Lipscomb, W. N. *J. Less Commun. Met.* **1981**, *82*, 1.
(9) Fehlner, T. P. *Adv. Inorg. Chem.* **1990**, *35*, 199.
(10) Lundström, T. In *Boron and Refractory Borides*; Matkovich, V. I., Ed.; Springer Verlag: Berlin, 1977.
(11) Hohnke, D.; Parthé, E. *Acta Crystallogr.* **1966**, *20*, 572.
(12) Joyner, D. J.; Johnson, O.; Hercules, D. M. *J. Am. Chem. Soc.* **1980**, *102*, 1910.

Table I. Mössbauer Parameters of an Amorphous Film Deposited from $B_2H_6Fe_2(CO)_6$ on Aluminum

T, K	δ,[a] mm/s	QS, mm/s	Γ, mm/s	ΔΓ, mm/s	$\langle H_{int}\rangle$,[b] kOe	% area	type of fit
297	0.19	0.00	0.40		82	100	P(H)
78	0.35	0.00	0.57		134	100	P(H)
297	0.20	0.03	0.65	0.90	75	100	1 sextet
78	0.37	0.07	0.65	1.68	134	100	1 sextet

[a] The isomer shift is relative to room temperature natural α-iron foil. [b] Average field.

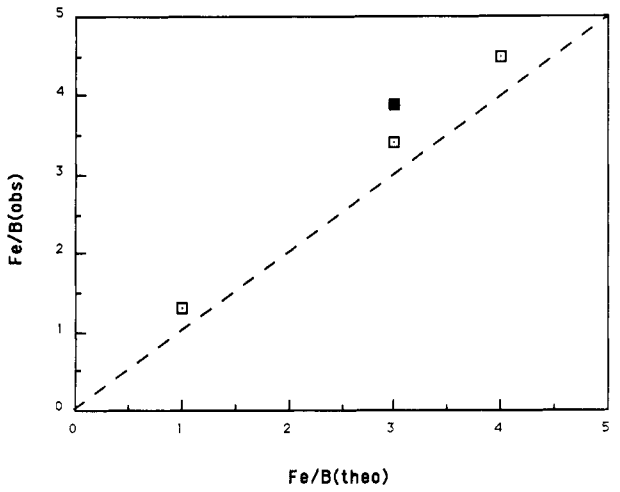

Figure 2. Plot of Fe/B (atom percent derived from Auger spectra, open squares; chemical analysis, closed square) vs Fe/B ratio of the molecular precursor. The straight line has a slope of 1.

experiment was carried out by placing a fine platinum mesh heated by contact with the substrate over the glass substrate surface. A contiguous film was still formed but with some surface texture due to the grid. Analysis revealed that its Fe/B ratio of 1.1 was closer to the ideal value and that both carbon and oxygen impurities were reduced to the 1–2% range. Thus, for this precursor a high-purity material with Fe/B = 1 should be attainable with suitable refinements of the deposition apparatus.

In Figure 2 the observed Fe/B ratios vs those expected from the three precursors, $B_2H_6Fe_2(CO)_6$, $HFe_3(CO)_9BH_4$, and $HFe_4(CO)_{12}BH_2$, are plotted for deposition at the lowest practical temperatures. Although the observed Fe/B trend follows the Fe/B ratio of the precursor cluster core, all the observed values are systematically high. The crystallization of the film formed from $HFe_3(CO)_9BH_4$ showed that, in this instance, that the high ratio is not an artifact of the Auger measurements.[3] As noted below, both the X-ray diffraction (XRD) and Mössbauer spectra results on the crystallized films, formed from $B_2H_6Fe_2(CO)_6$ and $[B_2H_4Fe_2(CO)_6]_2$, confirm that iron-rich films result from these precursors as well.

Properties. The film resistivity was measured for a uniform film of 1.5 cm × 0.6 cm × 6700 Å dimensions which was deposited from $B_2H_6Fe_2(CO)_6$ through a mask on a glass substrate upon which an equally spaced array of four gold electrodes had previously been deposited. Resistivity measurements by the four-point probe method[13] showed ohmic behavior over the current range 50–1000 μA and the resistivity calculated from the slope of the line was 234 μΩ cm at 22 °C. This is somewhat higher than typical values for metallic glasses[14] and is similar to that obtained for films formed from $HFe_3(CO)_9BH_4$. Clearly the integrity of the film is high and that the material is relatively pure.

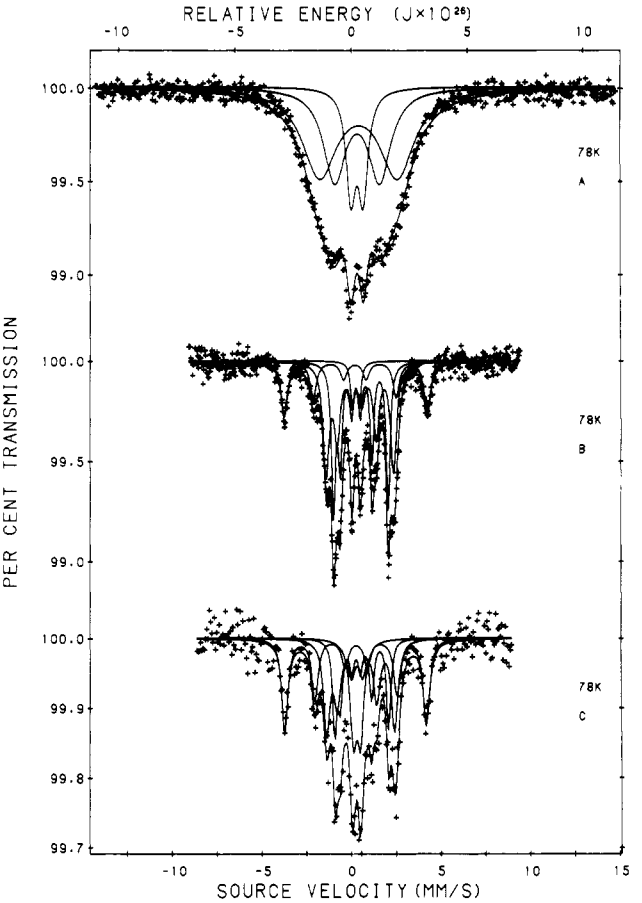

Figure 3. Mössbauer spectrum of an iron boride film produced from the deposition of $B_2H_6Fe_2(CO)_6$ on (A) iron-free aluminum foil and (B) quartz after crystallization at 600 °C for 48 h. (C) Mössbauer spectrum of an iron boride film produced from the deposition of $[B_2H_4Fe_2(CO)_6]_2$ on quartz after crystallization at 600 °C for 48 h. The parameters of the fits are given in Tables I and III.

Structure of the $B_2H_6Fe_2(CO)_6$-Derived Film. The XRD patterns of the thicker films, as deposited from $B_2H_6Fe_2(CO)_6$, exhibit very broad features that originate from the film and glass substrate. Hence, the films have no periodicity on the XRD scale and can be classified as amorphous materials. No α-Fe was detected.

Information on the existence of local structure around the iron atoms may be found in the Mössbauer spectra. The Mössbauer spectral parameters are complied in Table I for spectra run at 78 and 297 K and the 78 K spectrum is illustrated in Figure 3A. Consistent with the XRD data, there is no evidence for the presence of α-iron in the film. Hence, any iron in excess of that expected from the one to one Fe/B precursor ratio is part of the amorphous network. The broad spectral lines confirm the amorphous nature of the material and the magnetic sextet fit is consistent with a ferromagnetic material with a Curie temperature above room temperature. The substantial increase in the average hyperfine field between 297 and 78 K indicates that the Curie temperature is lower than that of a film formed from $HFe_3(CO)_9BH_4$. This is consistent

(13) Valdes, L. B. *Proc. IRE* **1954**, *42*, 420.
(14) Whittle, G. L.; Stewart, A. M.; Kaiser, A. B. *Phys. Status Solidi* **1986**, *97*, 199.

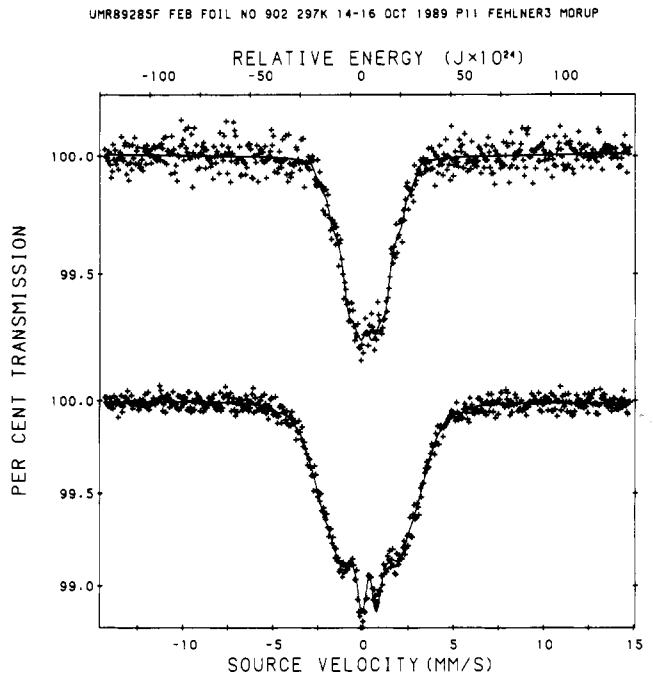

Figure 4. Mössbauer spectra obtained at 297 (top) and 78 K (bottom) of an iron boride film produced from the deposition of $B_2H_6Fe_2(CO)_6$ on iron-free aluminum foil and fit using the P(H) distribution shown in Figure 5.

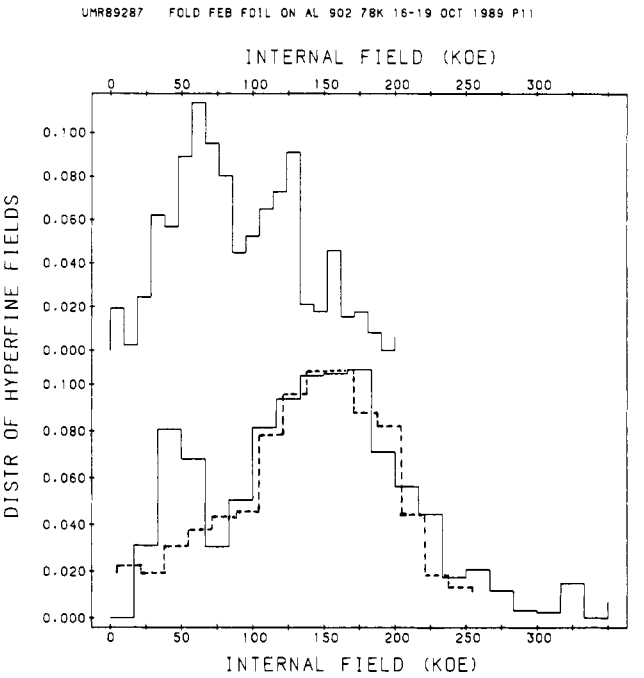

Figure 5. P(H) distribution (solid lines) found for the Mössbauer spectral fit shown in Figure 4 obtained at 297 (top) and 78 K (bottom). The dashed line corresponds to the P(H) distribution for the iron boride produced from the deposition of $HFe_3(CO)_9BH_4$ at 78 K shifted by 95 kOe to lower field.

with previous measurements of the Curie temperature as a function of boron content for sputtered iron–boron films.[5] As expected, the average hyperfine field is much lower than that of known iron–boron amorphous alloys with Fe/B ≥ 3 and is similar to that observed for crystalline FeB.[15] Qualitatively this is consistent with the film's composition because $\langle H_{int} \rangle$ decreases with increasing dilution of the magnetically active element. For this reason, the films cannot contain large amounts of hydrogen.

The $P(H)$ distribution of hyperfine fields, which reflects the distribution of iron environments, has been determined for this film. The resulting spectral fits are shown in Figure 4 and the corresponding $P(H)$ distributions are shown by the solid lines in Figure 5. Because of the rather small fields present at 297 K, the detailed structure shown in the distribution (Figure 5, top) probably is not real. However, at 78 K the spectrum is detailed enough to give a valid distribution (Figure 5, bottom). In this distribution the minor peak at ≈50 kOe is most likely the result of a paramagnetic component. Other work has demonstrated[16,17] that, for a totally random distribution of hard-sphere boron and iron atoms, the maximum of the $P(H)$ distribution should decrease and the width of the $P(H)$ distribution should increase with increasing boron content. Thus we can compare the $P(H)$ distribution for the film prepared from $B_2H_6Fe_2(CO)_6$ with that from the film prepared from $HFe_3(CO)_9BH_4$, a film which has half the boron content. The dashed line in Figure 5 is the $P(H)$ distribution for a film prepared from $HFe_3(CO)_9BH_4$. For comparison, this distribution has been shifted to lower hyperfine field strength by 95 kOe. Within experimental error, the two distributions are the same. A similar result has been reported for the comparison of $P(H)$ values for bulk ribbon samples prepared by the rapid quenching method; however, the composition range studied was $Fe_{75}B_{25}$ to $Fe_{85}B_{15}$.[17] The implication in both cases is that the amorphous films are not simply random mixtures of iron and boron atoms. A local structure about the iron atoms and, presumably, about the boron atoms exists. Unfortunately the Mössbauer spectra do not indicate the details of this structure in either case.

To learn more about the local structure, we have examined the crystallization behavior of the amorphous films. The rationale for such a study is that atomic motion induced on heating leads to an initial, perhaps metastable, crystalline phase that reflects the local structure in the amorphous state.[5,18] No evidence for crystallization was found by XRD at 400 or 500 °C and initial crystallization was observed at 600 °C, which is 200 °C higher than for films formed from $HFe_3(CO)_9BH_4$. XRD line patterns typical of a polycrystalline material were measured and the reflections are tabulated in Table II for a typical film. The diffraction pattern did not significantly change on further annealing either at 600 or at 700 °C (24 h). The assignments to known phases were made from published XRD data. All unassigned reflections are very weak. The two principal crystalline phases present are tetragonal Fe_2B and orthorhombic FeB as indicated in Table II. The presence of Fe_2B demonstrates that the Fe/B ratio in the amorphous thin films is greater than 1. The higher the substrate temperature during the film deposition, the greater was the amount of Fe_2B observed on crystallization. This is consistent with the Auger results and implies an increased loss of boron with increasing substrate temperature.

The same annealed sample used to obtain the XRD data given in Table II was examined by Mössbauer spectroscopy. To do so, the now-cracked film was pealed from the glass substrate, and the chips were placed in a matrix. The resulting Mössbauer spectral parameters obtained at 295 and 78 K are given in Table III, and the 78 K spectrum

(15) Takács, L.; Cadeville, M. C.; Vincze, I. *J. Phys. F.: Met. Phys.* **1975**, *5*, 800.
(16) Boudreaux, D. S. *Phys. Rev. B.* **1978**, *18*, 4039.
(17) Vincze, I.; Kemény, T.; Arajs, S. *Phys. Rev. B* **1980**, *21*, 937.
(18) Kemény, T.; Vincze, I.; Fogarassy, B.; Arajs, S. *Phys. Rev. B* **1979**, *20*, 476.

Table II. XRD Data after Crystallization at 600 °C of an Amorphous Film Deposited from $B_2H_6Fe_2(CO)_6$ on Quartz

2θ	d, Å	I/I_0, %	assignment
24.96	3.57	<3	Fe_2B
32.86	2.73	5	FeB.
37.84	2.38	75	FeB
38.90	2.32	8	FeB
41.35	2.18	8 br	FeB
42.90	2.11	3	Fe_2B
44.70	2.03	3	α-Fe(?)
45.22	2.00	79	Fe_2B, FeB
47.84	1.90	20	FeB
50.00	1.82	3	FeB
56.65	1.62	7	Fe_2B
57.80	1.60	15	FeB
63.16	1.47	100	FeB
63.36	1.47	69 sh	FeB
64.90	1.43	5	unk
72.86	1.30	10	FeB
73.00	1.30	5 sh	Fe_2B
73.86	1.28	<3	unk
76.58	1.24	3	FeB
77.35	1.23	6	FeB
77.56	1.23	5	FeB
78.06	1.22	7	FeB
79.92	1.20	5	Fe_2B, FeB
80.70	1.19	3	Fe_2B, FeB
82.82	1.16	29	FeB
94.75	1.05	<3	Fe_2B
98.70	1.02	<3	FeB
99.10	1.01	<3	FeB
107.87	0.954	<3	unk
112.75	0.926	<3	Fe_2B
113.8	0.920	<3	unk

is shown in Figure 3B. The absence of broad lines suggests that the extent of crystallization is high and that little, if any, amorphous material is present. Further, with the exception of a small amount of a paramagnetic component, the sample consists of two magnetic phases. No α-Fe is observed. The sextet with a magnetic hyperfine field of 235 kOe at 295 K has the same field, within experimental error, as the average reported at 295 K for authentic Fe_2B, i.e., Fe(I), 242.0 kOe and Fe(II), 231.7 kOe.[15] The pair of sextets of nearly equal intensities with 78 K hyperfine fields of 117 and 94 kOe have the same difference in field strengths as the two sextets found in authentic FeB (22.5 vs 22.7 kOe),[15] but in FeB the fields are significantly higher [Fe(I) 129.6 kOe and Fe(II) 106.9 kOe at 80 K]. The close agreement between the observed hyperfine field for the Fe_2B phase in the crystallized film and the literature values eliminates any instrumental calibration error as the source of the difference in the FeB fields. However, the results do indicate the presence of at least two iron sites that differ in the same way that the two sites in authentic FeB differ, but with lower overall hyperfine field strengths. As shown in Table III, further annealing at 700 °C results only in the partial conversion of the Fe_2B phase into the paramagnetic component which is presumed to be associated with oxidized iron.

The significantly lower hyperfine field observed for the "Fe_3B" phase formed in the crystallization of the amorphous film prepared by the deposition of $HFe_3(CO)_9BH_4$ was found to be due to the presence of a significant amount of a carbide impurity. That is, the actual phase formed was $Fe_3B_{1-x}C_x$, where x was as large as 0.4, and the lower hyperfine field strength follows from the fact that orthorhombic Fe_3B and Fe_3C have average hyperfine fields of 244 and 208 kOe, respectively. The 13-kOe lower hyperfine field for the "FeB" phase might also be attributed to the presence of carbon impurity in the phase. This hypothesis can be tested and eliminated. The Mössbauer spectrum gives the relative amount of each phase and, hence, one

Table III. Mössbauer Parameters after Crystallization of the Amorphous Films Deposited on Quartz

T, K	δ,[a] mm/s	QS, mm/s	H_{int}, kOe	line width, mm/s	% area
		From $B_2H_6Fe_2(CO)_6$			
295[b]	0.13	0.08	235	0.36	21
	0.26	0.18	106	0.33	34
	0.28	0.22	89	0.28	40
	0.16	0.32[b]	0	0.23	4
78[d]	0.22	0.07	247	0.42	20
	0.38	0.18	117	0.41	40[c]
	0.39	0.27	94	0.27	35[c]
	0.25	0.37[b]	0	0.25	5
78[e]	0.22	0.07	247	0.33	6
	0.39	0.13	123	0.35	33[c]
	0.40	0.28	97	0.35	46[c]
	0.25	0.43[b]	0	0.32	15
		From $[B_2H_4Fe_2(CO)_6]_2$			
78[d]	0.22	0.00	245	0.44	31
	0.38	0.21	117	0.44	32[c]
	0.38	0.34	92	0.33	23[c]
	0.29	0.40[b]	0	0.31	14

[a] The isomer shift is relative to room temperature natural α-iron foil. [b] The quadrupole splitting for the paramagnetic component. [c] An almost equally good fit to the spectra could be obtained if the areas of these two components were constrained to be equal. [d] Crystallized at 600 °C. [e] Heated further at 700 °C.

can calculate the composition for various assumed identities for the "FeB" phase. If the phase is pure FeB, then the overall Fe/B ratio calculated from the Mössbauer composition is 1.22 in good agreement with the Auger value of 1.32 for this particular film. Assuming the Auger values for carbon and oxygen contents are correct, the maximum amount of carbon that could be in this phase is 4 atom %. The boron thereby displaced should appear as oxidized boron. In the case of $Fe_3B_{1-x}C_x$ the boron displaced by carbon was identified as B_2O_3 by the characteristic Auger electron energy for oxidized vs unoxidized boron. However, in the present film the boron Auger electron peak shows no evidence of oxidized boron. Further, neither impurity level is large enough to account for the observed difference in the average of the fields. In addition, if significant carbon were present one would expect to see a rather broadened sextet resulting from a distribution of fields. Finally, incorporation of carbon is expected to change the unit cell parameters but the XRD results do not support such a conclusion. We conclude that the film does not incorporate a large enough carbon impurity that would be required to explain the significantly lower fields observed for the "FeB" phase in our film. Thus, we must seek some other explanation, to be proposed below.

Structure of the $[B_2H_4Fe_2(CO)_6]_2$-Derived Film. To provide additional information on the nature of the "FeB" phase resulting from the crystallization of the amorphous film produced from $B_2H_6Fe_2(CO)_6$, we sought a different precursor containing a cluster core with a Fe/B ratio of 1. If the kinetics of the deposition process are important in fixing the film structure and composition and if the rate-determining step were significantly different for the two precursors, one would expect to see a difference in the Fe/B ratio. Further, if the difference in the internal fields for the "FeB" phase in the film and in authentic FeB is structurally based, one would also expect to see a change in the fields for the crystallized film.

Our synthetic work has generated the molecule $[B_2H_4Fe_2(CO)_6]_2$ (Scheme II) which can now be prepared in good yield by the oxidative coupling of $[B_2H_4Fe_2(CO)_6]^{2-}$.[7] The internal cluster bonding is significantly different from that in $B_2H_6Fe_2(CO)_6$ in that there are fewer hydrogen ligands and a chain of four bonded boron atoms. If the rate-de-

termining step in deposition involves rupture of an iron to carbonyl ligand bond, then one might expect little difference in the final films. However, if the bonding in the cluster core is also involved, then differences in the solid-state products might be spectroscopically evident.

By using $[B_2H_4Fe_2(CO)_6]_2$ as a precursor, a film was deposited on a quartz substrate in the usual manner but somewhat above the minimum temperature for the smaller precursor. The film was amorphous by XRD and had carbon and oxygen impurity levels of ≈3% each. The film was then crystallized at 600 °C and examined by XRD and Mössbauer spectroscopy. The former demonstrated the presence of crystalline Fe_2B and FeB phases with the latter being predominant. The Mössbauer spectrum, shown in Figure 3c with the parameters of the fit given in Table III, has a poor signal-to-noise ratio because of small sample size but clearly is very similar to that found using $B_2H_6Fe_2(CO)_6$ as precursor. The only differences are the relative amount of the paramagnetic impurity and the ratio of the amounts of Fe_2B and "FeB" phases. The latter can be accounted for by the somewhat higher substrate temperature of 220 °C during deposition. Within experimental error the measured hyperfine field values are the same. Thus, one must conclude that the rate-determining step in the deposition process is not affected by the internal structure of the cluster precursor nor do the films show any measurable differences by XRD and Mössbauer spectroscopy. Unfortunately, this experiment does not answer the question of whether precursor structure is carried over into the solid state.

It does, however, place additional limits on the explanation for the low hyperfine fields for the "FeB" phase. It seems even more unlikely that the low fields can be associated with an impurity problem because the discrepancy would be expected to depend on impurity levels which are different in the two cases. One possible impurity, of which we have no direct measure, is hydrogen. The presence of hydrogen could result in lower fields, but the amount of hydrogen is unlikely to be identical for films formed from the two precursors and, further, it is difficult to explain why all the hydrogen would be segregated into the "FeB" phase with little in the Fe_2B phase. The presence of a large amount of hydrogen is also inconsistent with the measured resistivities. Therefore, we conclude that the reduced fields are an intrinsic characteristic of the material prepared by our method and the difference between the bulk values and those for our films resides in a difference in magnetic structure. One possible explanation may be that the crystallized FeB phase is coated with the Fe_2B phase. If the easy magnetic axis in the Fe_2B phase is opposed to that in the FeB phase, the transferred field experienced by the FeB iron moments would vectorially subtract from the intrinsic moments in FeB. This could result in the lowering of the two fields in FeB by the same 13 kOe. The effect of FeB on Fe_2B is expected to be smaller because of the much lower hyperfine field of the former. A similar type of "superferrimagnetic" coupling has been proposed between goethite crystals.[19]

Discussion and Conclusions

Consistent with our earlier results on ferraborane clusters, $B_2H_6Fe_2(CO)_6$ and $[B_2H_4Fe_2(CO)_6]_2$ serve as equivalent precursors for an iron boride film with an Fe/B ratio close to 1. This demonstrates that discrete ferraboranes provide an approach to film stoichiometries not accessible via the rapid quenching techniques. Under the mild conditions employed, amorphous materials are produced with relatively minor carbon and oxygen impurities. The $P(H)$ distributions resulting from an analysis of the Mössbauer spectra demonstrate the existence of local structure. The compatibility of short-range order without the presence of long-range order has been described previously.[20] Because the most common description of the crystalline structures of metal rich borides is based on face-capped boron centered trigonal prisms of metals,[21] it is not obvious how $B_2H_6Fe_2(CO)_6$ and $[B_2H_4Fe_2(CO)_6]_2$ can lead to an amorphous material that crystallizes to known phases without the total loss of the internal cluster structure. However, alternate descriptions of solid-state structures exist, and Matkovich has provided a description of the structure of orthorhombic FeB that is based on a Fe_2B_2 tetrahedron as the repeating unit.[22] This is reproduced in Figure 6 along with a cartoon representation of the amorphous state as a random array of Fe_2B_2 tetrahedran generated by stripping the CO and H_2 ligands from $B_2H_6Fe_2(CO)_6$. This crystallization "model" seems satisfying even if we have no evidence to support its detail.

Figure 6 contains a representation of the structure of FeB emphasizing a plane in the a and c crystallographic directions. In the b direction, Figure 7, the existence of extended B–B chains becomes evident. The representation in terms of Fe_2B_2 tetrahedra also shows that $B_2H_6Fe_2(CO)_6$ is a molecular form of the basic building block, whereas $[B_2H_4Fe_2(CO)_6]_2$ is a molecular form of two such building blocks, joined in a manner very similar to that in Figure 7. Both the structure of FeB and CrB can be viewed as being built up of chains of tetrahedra as shown in Figure 7. These two structures differ in the manner in which the chains pack. As mentioned above, polymorphism of some metal silicides and germanides involving the FeB and CrB structural types is known.[11] This was an additional reason for utilizing the two different precursors in order to determine if different structural forms might be adopted on crystallization of the amorphous films. In fact, both precursors resulted in the same crystalline form of FeB even though there are reports in the early literature of a second form of FeB.[23] On the other hand, the magnetic behavior of the mixed phases is distinctly different and can be attributed to the method of preparation.

Experimental Section

The $B_2H_6Fe_2(CO)_6$ cluster was prepared by the reaction of $Fe_2(CO)_9$ with $BH_3{\cdot}SMe_2$ and was purified by fractionation.[24] $[B_2H_4Fe_2(CO)_6]_2$ was prepared by the oxidative coupling of $[B_2H_4Fe_2(CO)_6]^{2-}$ with $FeCl_2/FeCl_3$ and purified by column chromatography.[25] To prepare a film, the liquid $B_2H_6Fe_2(CO)_6$ was evaporated at 22 °C, or $[B_2H_4Fe_2(CO)_6]_2$ was sublimed at 40 °C in the low-pressure CVD reactor described previously.[2] In the former case, the solid sublimer was replaced with a simple tube leading to the Schlenk tube containing the precursor. Typical deposition times were 15–20 min. The substrates were resistively heated and the temperature was monitored by a 0.005-in.-diameter iron/constantan thermocouple held in place on the outer face of the substrate surface by the substrate-heater clamp. $B_2H_6Fe_2(CO)_6$ was deposited at several temperatures and the lowest practical temperature was found to be 170 °C. $[B_2H_4Fe_2(CO)_6]_2$ was deposited at 225 °C. The temperature of the substrate surface measured by the thermocouple increased 5–10 °C during the deposition of the highly reflective films. The reactor was evac-

(19) Mørup, S.; Madsen, M. B.; Franck, J.; Villadsen, J.; Koch, C. J. W. *J. Magn. Magn. Mater.* **1983**, *40*, 163.
(20) Sanchez, R. H.; Zhang, Y. D.; Budnick, J. I.; Hasegawa, R. *J. Appl. Phys.* **1989**, *66*, 1671.
(21) Greenwood, N. N.; Parish, R. V.; Thorton, P. *Q. Rev.* **1966**, *20*, 441.
(22) Matkovich, V. I. *Pure Appl. Chem.* **1974**, *39*, 525.
(23) Wever, F.; Müller, A. *Mitt. K. W. Inst. Eisenforsch.* **1929**, *11*, 197.
(24) Meng, X.; Fehlner, T. P. *Inorg. Synth.* **1992**, *29*, 0000.
(25) Jun, C.-S.; Fehlner, T. P., unpublished work.

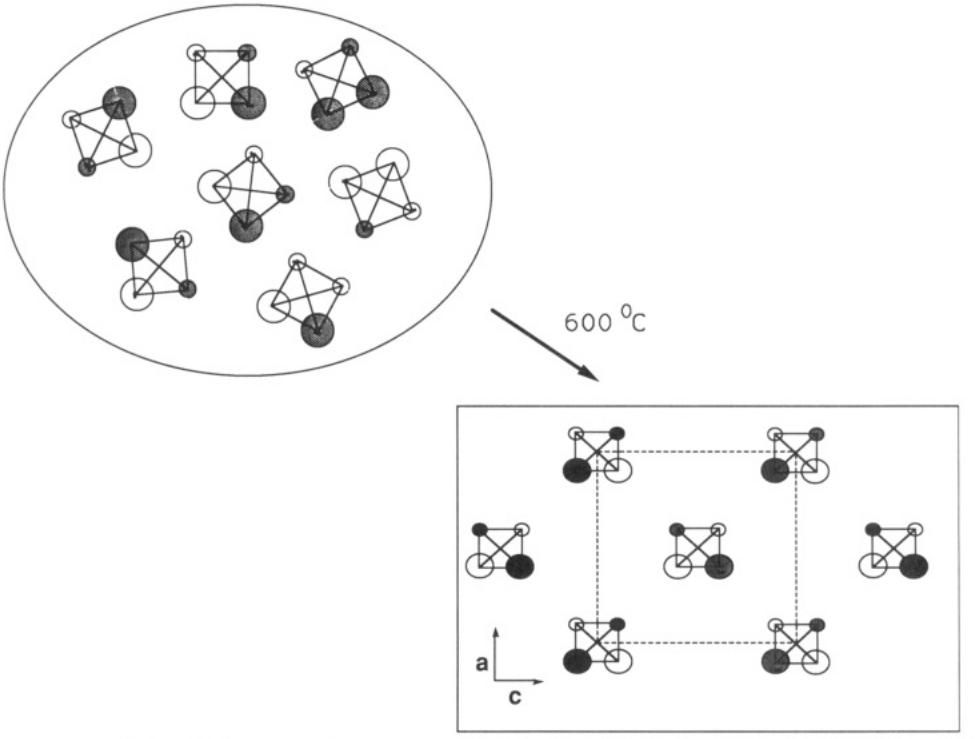

Figure 6. Cartoon representation of the conversion of amorphous iron boride produced by the deposition of $B_2H_6Fe_2(CO)_6$ into orthorhombic FeB. The latter representation is due to Matkovich,[22] and the small and large circles represent B and Fe, respectively, the solid circles represent $y = {}^3/_4$, the empty circles $y = {}^1/_4$, and the shaded circles $y = -{}^1/_4$.

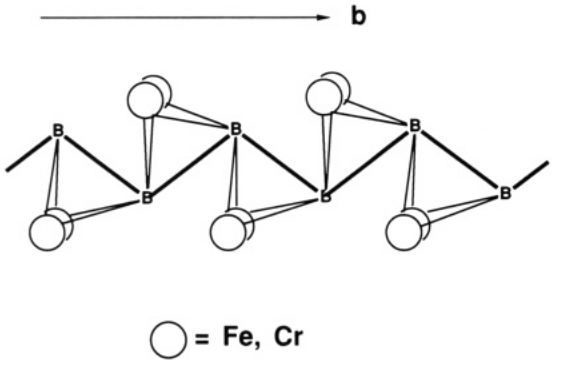

Figure 7. Representation of the chains of Fe_2B_2 tetrahedra present in both FeB and CrB along the *b* crystallographic direction in orthorhombic FeB.

uated with a turbomolecular pump and ion pump and a base pressure of 2×10^{-8} Torr was achieved after heating overnight at ≈60 °C. During deposition, total pressures were $\approx 10^{-5}$–10^{-4} Torr. A mass spectrometer downstream of the substrate was used to monitor the production of CO and H_2. Depositions were carried out on glass substrates (Corning 7059 or quartz, 2×2.5 cm) and, for the Mössbauer studies of the amorphous film, on an iron-free aluminum foil which covered a glass substrate. Film thicknesses were measured with a Tencor profilometer and resistivities were measured by the four-point method.

The films deposited on quartz were annealed in a quartz tube which was heated with a tube furnace under a vacuum of 10^{-6} Torr. Annealing temperatures stated are furnace temperatures, and no attempt was made to measure the threshold temperatures for crystallization. Although the films in the amorphous state adhered well to the glass substrate, after crystallization the surface was cracked and the thicker films pealed away from the substrate. The crystallinity was assayed with a Philips 3520 X-ray powder diffraction system.

Auger spectra were obtained on a Perkin-Elmer 590 Auger multiprobe with 3-kV electrons after sputtering with 4-kV Ar^+ (1 mm^2 spot) at 100 Å/min to constant composition (≤200 Å). Beam currents of 3.8 μA were used. Spectra from a foil standard ($Fe_{81}B_{13.5}Si_{3.5}C_2$) were gathered with each unknown sample, and these data were used to calculate sensitivities for Fe, B, and C. The sensitivity for O relative to that of C was the standard instrument value for the electron energy used. The variation in atom sensitivities from experiment to experiment was small.

The Mössbauer effect spectra were obtained at 297 and 78 K on a constant acceleration spectrometer which utilized a room-temperature rhodium-matrix ^{57}Co source and was calibrated at room temperature with natural-abundance α-iron foil. The Mössbauer spectra were fit either with magnetic sextets or with a distribution of hyperfine fields.[26] In the magnetic sextet fits the individual components were constrained to the ratio of 3:2:1:1:2:3, as would be expected for a sample with no texture, and the line widths were constrained in the ratio $\Gamma + \Delta\Gamma{:}\Gamma + 0.5\Delta\Gamma{:}\Gamma{:}\Gamma + 0.5\Delta\Gamma{:}\Gamma + \Delta\Gamma$. For the crystallized samples $\Delta\Gamma$ was found to be zero. The fits shown in Figure 4 assume that no texture is present in the amorphous films. Fits to these spectra with components in the ratio $3{:}x{:}1{:}1{:}x{:}3$, where x is between 1 and 2, were almost as good as those shown in Figure 4. Hence, the Mössbauer fits cannot eliminate the presence of texture as was found in our earlier work on the Fe_3B based amorphous thin films.[2]

Acknowledgment. The support of the Army Research Office (TPF), the National Science Foundation (TPF), and the donors of the Petroleum Research Fund, administered by the American Chemical Society (GJL) are gratefully acknowledged.

Registry No. Fe_2B, 12006-85-8; FeB, 12006-84-7; $B_2H_6Fe_2(CO)_6$, 67517-57-1; $[B_2H_4Fe_2(CO)_6]_2$, 133128-57-1; $Fe_{56}B_{44}$, 138858-31-8.

(26) Wivel, C.; Mørup, S. *J. Phys. E.: Sci. Instrum.* **1981**, *14*, 605.